Korean J. Chem. Eng., 36(3), 356-367 (2019)
DOI: 10.1007/s11814-018-0215-5

pISSN: 0256-1115
eISSN: 1975-7220

Analytical design of constraint handling optimal two parameter internal model control for dead-time processes

Rodrigue Tchamna[*,,‡], Muhammad Abdul Qyyum[*,‡], Muhammad Zahoor[*,‡], Camille Kamga[**], Ezra Kwok[***], and Moonyong Lee[*,†]**

*School of Chemical Engineering, Yeungnam University, Gyeongsan 38541, Korea
**University Transportation Research Center, City College of New York, New York 10031, U.S.A.
***Chemical & Biological Engineering, University of British Columbia, Vancouver, Canada
(*Received 15 September 2018 • accepted 18 December 2018*)

Abstract–This work presents an advanced and systematic approach to analytically design the optimal parameters of a two parameter second-order internal model control (IMC) filter that satisfies operational constraints on the output process, the manipulated variable as well as rate of change of the manipulated variable, for a first-order plus dead time (FOPDT) process. The IMC parameters are designed to minimize a control objective function composed of the weighted sum of the error between the process variable and the set point, and the rate of change of the manipulated variable, and to satisfy the desired constraints. The feasible region of the constrained IMC control parameters was graphically analyzed, as the process parameters and the constraints varied. The resulting constrained IMC control parameters were also used to find the corresponding industrial proportional-integral controller parameters of a Smith predictor structure.

Keywords: Optimal IMC Control, Operational Constraints, Constrained Optimization, Analytical Design Approach, Constraint Handling

INTRODUCTION

Robust control design has been of great interest in many research fields, including chemical engineering, where processes are inherently doomed to uncertainties [1,2]. Most chemical manufacturing processes are controlled by proportional-integral-derivative (PID) controllers. Although PID control is the most used control algorithm in industry, the tuning of optimal PID parameters can sometimes be a daunting challenge. The stability analysis of a classical PID controller is even more demanding for a system with time delay. To overcome this challenge, many researchers have developed other control methods for time delay systems, based on the performance of a desired closed-loop response. The direct synthesis (DS) method [3] and the internal model control-PID (IMC-PID) tuning methods [4-8] are two examples of such tuning method. The IMC-PID method mainly focuses on the tuning of the PID parameters rather than the design of the IMC parameters itself [9]. Its most attractive feature is that it usually has only one tuning parameter instead of three for the classical PID controller. The relation between the IMC parameter and the PID controllers has largely been discussed in the above-mentioned references, either for set point tracking or disturbance rejection. However, little has been done when it comes to the choice of the optimal IMC filter parameters. Unlike previous papers that mainly focused on the design of the IMC-PID, we focus on the design of the optimal parameters of a second-order internal model control (IMC) filter that satisfies operational constraints on the output process, the manipulated variable and the rate of change of the manipulated variable, for the first-order plus dead time (FOPDT) process. The choice of FOPDT system is motivated by the fact that, for the sake of control system design, higher-order processes can be successfully reduced to a standard FOPDT system that captures most of the dynamics of industrial plants. For the simplification of design of the IMC parameter, previous research about the IMC usually prefers to tune only one parameter. The guideline for choosing this adjustable IMC parameter is usually roughly given in terms of the process time constant and time delay, or selection of the parameter is based on the desired level of robustness, measured by the peak of the maximum sensitivity M_s [4]. Ghousiya et al. [10] graphically presented the relation between the maximum sensitivity and the filter parameter, for various type of systems. Zhao et al. proposed a clear designing and parameter tuning approach of IMC-PID controller for the first-order plus time-delay (FOPTD) process and the second-order plus time-delay (SOPTD) process and used an analytically designed the filter parameter based on the maximum sensitivity of the system [9]. One of the few papers based on the optimal control of IMC parameter based on the integral square error performance index is that of Kang Liu et al. [11]. The authors designed the IMC parameter based on a performance index defined as the integral square error (ISE) and the maximum of the complementary sensitivity function. The performance index was graphically plotted in terms of the filter parameter and the minimum of the performance index was graphically found. The drawback in their method is that the performance index did not include the variation of the control law (manipulated variable), and also, graphical methods are good for offline control computation, but for online control design,

†To whom correspondence should be addressed.
E-mail: mynlee@yu.ac.kr
‡These authors contributed to this work equally.

analytical method are highly desired.

It is also well-known that the tuning of a single IMC parameter results in the inherent trade-off between small value of the parameter (faster response) and large value of the parameter (sluggish but robust response), whereas a two parameter second-order IMC filter may bring about more design flexibility. In fact, the only benefit of using a single parameter IMC instead of multi parameters is that dealing with only one control variable is simpler than that having multiple tuning variables. However, on the other hand, for control robustness, having multiple control variables brings more degree of freedom, hence, more flexibility to the control design and helps reducing the unavoidable inherent tradeoff issue that exists in control system design. The single parameter IMC controller was long preferred for its design simplicity. The present paper brings a new contribution by removing the design complexity of a two parameter IMC filter, by clearly addressing the design of the two optimal filter control parameters, in a closed-form, getting rid of the time-consuming burden brought about by the trial and error steps, and with the additional benefit of satisfying all the operational constraints imposed to the system. In the current paper, a two parameter second-order IMC filter is designed based on the ISE performance index, comprising the weighted sum of the error between set point and process variable and the rate of change of the manipulated variable subjected to operational constraints: maximum allowable process variable, maximum allowable manipulate variable and maximum allowable rate of change in the manipulate variable. In this way, two resulting IMC parameters will satisfy the minimization of the process variable and manipulated variable, while satisfying the system constraints.

PRINCIPLE OF THE IMC CONTROL

As stated by Riviera et al., the objective of the IMC controller is to benefit from the ease and simplicity of an open loop controller design, while retaining the benefits of a feedback system [4]. The close loop transfer function of the system is shown in Fig. 1

$$Y = \frac{qG}{1+q(G-\tilde{G})}Y_{sp} + \frac{1-q\tilde{G}}{1+q(G-\tilde{G})}D \tag{1}$$

$$U = \frac{q}{1+q(G-\tilde{G})}(Y_{sp}-D) \tag{2}$$

where Y is the process variable, G the process transfer function, $\tilde{G}$ the plant model, q the IMC controller transfer function, Y_{sp} the set point, and D the output disturbance.

For servo system (D=0) and perfect model ($G \approx \tilde{G}$), Eq. (1) is reduced to

$$Y = q\tilde{G}Y_{sp} \tag{3}$$
$$U = qY_{sp}$$

The objective of IMC for ideal tracking is to achieve $Y=Y_{sp}$. To this end, the product $q\tilde{G}$ in Eq. (3) should be equal to unity. So, the IMC controller q should be the inverse of the plant model, $\tilde{G}^{-1}$. However, we need to make sure that the controller is not only causal (i.e., proper), but also stable. Thus, the model needs to be factored as [4]

$$\tilde{G} = P_M P_A \tag{4}$$

where P_A contains all non-minimal (maximum) phase elements of the plant model: any time delays and right-half plane zeros. Besides, the steady state gain of P_A, $P_A(0)$ should be equal to one, to ensure no steady state for step reference or disturbance change. P_M contains all minimal phase elements of the plant model, the inverted part of the model. The controller is chosen as

$$q = P_M^{-1} f \tag{5}$$

where f is the filter, designed to make the controller proper. Plugging Eqs. (4) and (5) into the expression of Y and U in Eq. (3) yields

$$Y = P_A f Y_{sp} \tag{6}$$
$$U = P_M^{-1} f Y_{sp}$$

For an FOPDT with perfect model,

$$G = \tilde{G} = \frac{K}{\tau s+1} e^{-\theta s} \tag{7}$$

The factorization of Eq. (7) as suggested by Eq. (4) yields

$$P_M = \frac{K}{\tau s+1};\ P_A = e^{-\theta s} \tag{8}$$

The closed-loop transfer functions in Eq. (6) become

$$\frac{Y}{Y_{sp}} = f e^{-\theta s}$$
$$\frac{U}{Y_{sp}} = \frac{\tau s+1}{K} f \tag{9}$$

For design simplicity, it is a common practice to choose only one single tuning filter parameter. However, for more design flexibility,

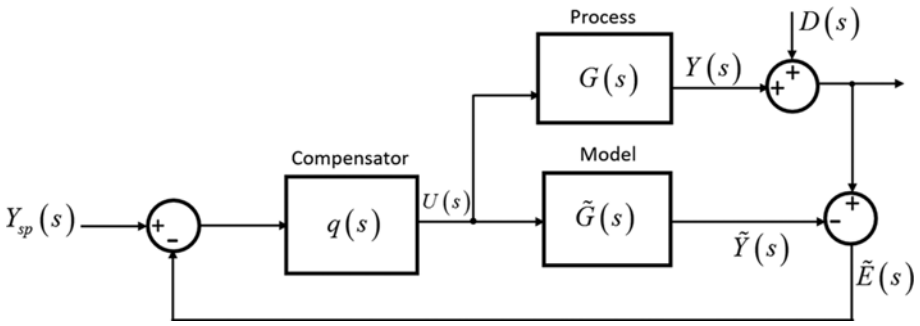

Fig. 1. IMC structure for a general stable dynamic system with output disturbance.

a general form of the filter f, for unstable processes, is usually under the form [12],

$$f=\frac{\Sigma_{i=1}^{m}\beta_i s^i+1}{(\lambda^2 s^2+2\lambda\zeta s+1)^r} \tag{10}$$

where the m zeros of the filter, β_i are designed to cancel the m unstable poles of the process, while r is chosen large enough to make the controller $q=P_M^{-1}f$ proper/causal. λ and ζ are the time constant and the damping ratio of the filter, respectively. For simplification purpose and focus on the designing of the constraint optimal controller, the second-order filter selected in this study is as follows:

$$f=\frac{1}{\lambda_1 s^2+\lambda_2 s+1} \tag{11}$$

where $\lambda_1>0$ and $\lambda_2>0$ are two independent parameters. For the sake of having some meaningful physical interpretation, the general second-order filter in Eq. (11) can be converted into the following standard second order system:

$$f=\frac{1}{\lambda_1 s^2+\lambda_2 s+1}=\frac{1}{\tau_c^2 s^2+2\zeta\tau_c s+1} \tag{12}$$

where τ_c is the filter time constant and ζ the filter damping ratio. Eqs. (11) and (12) yield the following relations:

$$\begin{aligned}\tau_c&=\sqrt{\lambda_1}\\ \zeta&=\frac{\lambda_2}{2\sqrt{\lambda_1}}=\frac{1}{2}\sqrt{\frac{\lambda_2^2}{\lambda_1}}\end{aligned} \tag{13}$$

The objective of the paper is to design to coefficients λ_1 and λ_2 or τ_c and ζ, such as that the control system is not only optimal, but also satisfies all the constraints requirement on y_{max}, u_{max} and u'_{max}. Substituting the value of the filter in Eq. (12) into Eq. (9) yields

$$\begin{aligned}Y&=\frac{1}{\tau_c^2 s^2+2\zeta\tau_c s+1}Y_{sp}e^{-\theta s}\\ U&=\frac{\tau s+1}{K}\frac{1}{\tau_c^2 s^2+2\zeta\tau_c s+1}Y_{sp}\end{aligned} \tag{14}$$

Since the delay term $e^{-\theta s}$ that appears in Eq. (14) is in the numerator, the control system can be designed using only the free part of the system, and then the actual system including dead-time is same as the dead-time free system, with a time shift that amounts to the value of the dead-time. Let's define the dead-time free system as,

$$\begin{aligned}Y^*&=\frac{1}{\tau_c^2 s^2+2\zeta\tau_c s+1}Y_{sp}\\ U&=\frac{\tau s+1}{K}\frac{1}{\tau_c^2 s^2+2\zeta\tau_c s+1}Y_{sp}\end{aligned} \tag{15}$$

For simplicity, the star (*) will be dropped on y in the remainder of this paper, and the notation y will be considered as the dead-time free part of the system.

PROBLEM FORMULATION

1. Formulation of Constrained IMC Optimal Control

After introducing the principle of the IMC controller in the previous section, this section provides the formulation of the main contribution of this paper. The main idea of the IMC parameters design in this paper is to improve the previous design that where roughly giving the filter parameter in terms of the plant parameters and the dead-time of the system, based on the desired level of robustness, measured by the peak of the maximum sensitivity M_s [4]. In this paper, the IMC filter parameters are designed such that the following performance index is minimized

$$\min \Phi=\omega_y\int_0^\infty (e(t))^2 dt+\omega_u\int_0^\infty (u'(t))^2 dt \tag{16}$$

subject to

$$|y(t)|\le y_{max} \tag{17-1}$$

$$|u'(t)|\le u'_{max} \tag{17-2}$$

$$|u(t)|\le u_{max} \tag{17-3}$$

where

$$e(t)=y(t)-y_{sp}(t) \tag{18}$$

To be able to analytically solve the optimum solution of the problem defined in Eqs. (16) to (18), the analytical solutions of the y(t), u(t) and u′(t) are first derived and given in Appendix (A1) to (A3). Eq. (17-1) is satisfied for every value of time if the peak value of y(t), y_{peak}, is less or equivalent to maximum allowable value of the process variable, y_{max}. Likewise, Eq. (17-2) is satisfied for every value of time if the peak value of u(t), u_{peak}, is less or equal to the maximum allowable value of the manipulated variable, u_{max}. The same reasoning can be made for Eq. (17-3). Therefore, Eqs. (17-1) to (17-3) can yield the following constraints:

$$|y_{peak}|\le y_{max}\Rightarrow g(\zeta)\le\gamma_g \tag{19-1}$$

$$|u_{peak}|\le u_{max}\Rightarrow f(\zeta,\ \tau_c)\le\gamma_f \tag{19-2}$$

$$|u'_{peak}|\le u'_{max}\Rightarrow h(\zeta,\ \tau_c)\le\gamma_h \tag{19-3}$$

where

$$\gamma_g=\left|\frac{y_{max}}{\Delta Y_{sp}}\right|;\ \gamma_f=\left|\frac{Ku_{max}}{\Delta Y_{sp}}\right|\gamma_h=\left|\frac{Ku'_{max}}{\Delta Y_{sp}}\right| \tag{20}$$

The functions $g(\zeta)$, $f(\zeta,\ \tau_c)$ and $h(\zeta,\ \tau_c)$ are given in Appendices (B3), (B6) and (B12), respectively. The exact solution of the performance index (objective function) in Eq. (16) can be found as,

$$\phi=\alpha_{\phi_y}\frac{\tau_c}{\zeta}(4\zeta^2+1)+\alpha_{\phi_u}\frac{\tau^2+\tau_c^2}{\tau^2\zeta\tau_c^3} \tag{21}$$

with

$$\alpha_{\phi_y}=\frac{\omega_y\Delta Y_{sp}^2}{4};\ \alpha_{\phi_u}\frac{\omega_u\Delta Y_{sp}^2\tau^2}{4K^2} \tag{22}$$

2. Constrained Optimal IMC Design

With the constraints on the process variable, manipulated variable and the rate of the manipulated variable expressed in Eq. (19), the objective function of the constrained optimal control problem can be defined as follows:

$$\begin{aligned}L(\tau_c,\ \zeta,\ \varpi_1,\ \varpi_2,\ \varpi_3,\ \sigma_1,\ \sigma_2,\ \sigma_3)&=\phi+\varpi_1(\gamma_h-h(\zeta,\ \tau_c)-\sigma_1^2)\\ &+\varpi_2(\gamma_g-g(\zeta)-\sigma_2^2)+\varpi_3(\gamma_f-f(\zeta,\ \tau_c)-\sigma_3^2)\end{aligned} \tag{23}$$

where $\varpi_1>0$, $\varpi_2>0$, $\varpi_3>0$ are the Lagrange multipliers and σ_1, σ_2, σ_3 are slack variables. The conditions essential for optimum results

are as follows:

$$\frac{\partial \mathrm{L}}{\partial \tau_c}=\frac{\partial \phi}{\partial \tau_c}+\varpi_1\left(-\frac{\partial \mathrm{h}(\zeta,\ \tau_c)}{\partial \tau_c}\right)+\varpi_3\left[-\frac{\partial \mathrm{f}(\zeta,\ \tau_c)}{\partial \tau_c}\right]=0 \tag{24}$$

$$\frac{\partial \mathrm{L}}{\partial \zeta}=\frac{\partial \phi}{\partial \zeta}-\varpi_1\frac{\partial \mathrm{h}(\zeta,\ \tau_c)}{\partial \zeta}-\varpi_2\frac{\partial \mathrm{g}(\zeta)}{\partial \zeta}-\varpi_3\frac{\partial \mathrm{f}(\zeta,\ \tau_c)}{\partial \zeta}=0 \tag{25}$$

$$\frac{\partial \mathrm{L}}{\partial \varpi_1}=\gamma_h-\mathrm{h}(\zeta,\ \tau_c)-\sigma_1^2=0 \tag{26}$$

$$\frac{\partial \mathrm{L}}{\partial \varpi_2}=\gamma_g-\mathrm{g}(\zeta)-\sigma_2^2=0 \tag{27}$$

$$\frac{\partial \mathrm{L}}{\partial \varpi_3}=\gamma_f-\mathrm{f}(\zeta,\ \tau_c)-\sigma_3^2=0 \tag{28}$$

$$\frac{\partial \mathrm{L}}{\partial \sigma_1}=-2\,\varpi_1\sigma_1=0;\ \frac{\partial \mathrm{L}}{\partial \sigma_2}=-2\,\varpi_2\sigma_2=0;\ \frac{\partial \mathrm{L}}{\partial \sigma_3}=-2\,\varpi_3\sigma_3=0 \tag{29}$$

Case A ($\varpi_1=\varpi_2=\varpi_3=0$): The maximum point, ($\zeta^{\dagger}$, $\tau_c^{\dagger}$) is the global optimum in this case, and is situated in the feasible region. By solving Eqs. (24) and (25), it can be obtained as,

$$\begin{aligned}\tau_c^{\dagger}&=\left(\frac{\alpha_{\phi_u}}{\alpha_{\phi_y}}\right)^{\frac{1}{4}}=\left(\frac{\omega_{u'}\tau^2}{\omega_y \mathrm{K}^2}\right)^{\frac{1}{4}}=\left(\frac{\omega_{u'}}{\omega_y}\right)^{\frac{1}{4}}\sqrt{\frac{\tau}{\mathrm{K}}}\\ \zeta^{\dagger}&=\left[\frac{1}{4\tau^2}\left(\frac{\alpha_{\phi_u}}{\alpha_{\phi_y}}\right)^{\frac{1}{2}}+\frac{1}{2}\right]^{\frac{1}{2}}=\left[\frac{1}{4\tau^2}\left(\frac{\omega_{u'}\tau^2}{\omega_y \mathrm{K}^2}\right)^{\frac{1}{2}}+\frac{1}{2}\right]^{\frac{1}{2}}\end{aligned} \tag{30}$$

The optimal values of the IMC parameters can be elaborated in terms of λ_1 and λ_2 as follows:

$$\begin{aligned}\lambda_1^{\dagger}&=(\tau_c^{\dagger})^2=\sqrt{\frac{\omega_{u'}}{\omega_y}}\frac{\tau}{\mathrm{K}}\\ \lambda_2^{\dagger}&=2\,\tau_c^{\dagger}\zeta^{\dagger}=2\left(\frac{\omega_{u'}}{\omega_y}\right)^{\frac{1}{4}}\sqrt{\frac{\tau}{\mathrm{K}}}\left[\frac{1}{4\tau^2}\left(\frac{\omega_{u'}\tau^2}{\omega_y \mathrm{K}^2}\right)^{\frac{1}{2}}+\frac{1}{2}\right]^{\frac{1}{2}}\end{aligned} \tag{31}$$

Case B ($\sigma_1=\varpi_2=\varpi_3=0$): The global optimum, ($\zeta^{*h}$, τ_c^{*h}), is on the active constraint, $\gamma_h-\mathrm{h}(\zeta,\ \tau_c)$. For $\mathrm{h}(\zeta,\ \tau_c)=\frac{\tau}{\tau_c^2}$ as defined in Eq. (B12-1) in appendix, the optimal solution in this case can be obtained as,

$$\begin{cases}\tau_c^{*h}=\sqrt{\dfrac{\tau}{\gamma_h}}\\ \zeta^{*h}=\dfrac{\sqrt{\tau\omega_y[\mathrm{K}^2\tau\omega_y+(\gamma_h\tau+1)\gamma_h\omega_{u'}]}}{2\mathrm{K}\tau\omega_y}\end{cases} \tag{32}$$

Case C ($\sigma_2=\varpi_1=\varpi_3=0$): The global optimum, ($\zeta^{*g}$, τ_c^{*g}), is located on the active constraint, $\gamma_g-\mathrm{g}(\zeta)=0$. Since the function g only depends on ζ, and γ_g is a constant, the solution of $\gamma_g-\mathrm{g}(\zeta)=0$ is the minimum allowable damping ratio ζ_{min} of the IMC filter. (ζ^{*g}, τ_c^{*g}) can be found by solving the following system of equations:

$$\begin{cases}\zeta^{*g}=\zeta_{min}=-\dfrac{\log(\gamma_g-1)}{\sqrt{[\log(\gamma_g-1)]^2+\pi^2}}\\ \tau_c^{*g}=\left(\dfrac{\alpha_{\phi_u}+\sqrt{\alpha_{\phi_u}^2+12\,\alpha_{\phi_u}\alpha_{\phi_y}\tau^4(4\zeta_{min}^2+1)}}{2\alpha_{\phi_y}\tau^2(4\zeta_{min}^2+1)}\right)\end{cases} \tag{33}$$

The minus sign in the expression of ζ_{min} in Eq. (33) means that, for ζ_{min} to be a positive value, the argument of the logarithmic function should be less than one, so the logarithm function becomes negative.

$$\zeta_{min}>0\Rightarrow 0<\gamma_g-1<1 \tag{34}$$

Substituting the expression of γ_g in Eq. (20) into Eq. (34), Eq. (34) yields the following condition:

$$\Delta \mathrm{Y}_{sp}<\mathrm{y}_{max}<2\Delta \mathrm{Y}_{sp} \tag{35}$$

The condition in Eq. (35) is a well-known condition: the peak of the process variable is greater than the set point change and less than two-times the amplitude of the set point change. This guarantees that ζ_{min} will always be a positive value.

Case D ($\sigma_1=\sigma_2=\varpi_3=0$): The global optimum, ($\zeta^{gh}$, τ_c^{gh}), is on the peak point delimited by $\gamma_g-\mathrm{g}(\zeta)=0$ and $\gamma_h-\mathrm{h}(\zeta,\ \tau_c)=0$. Solving the following equations will provide the optimum solutions:

$$\begin{cases}\gamma_g-\mathrm{g}(\zeta)=0\\ \gamma_h-\mathrm{h}(\zeta,\ \tau_c)=0\end{cases} \tag{36}$$

For $\mathrm{h}(\zeta,\ \tau_c)=\frac{\tau}{\tau_c^2}$ as defined in Eq. (B12-1) in the appendix, the optimal solution in this case can be obtained as,

$$\begin{cases}\zeta^{gh}=\zeta_{min}=-\dfrac{\log(\gamma_g-1)}{\sqrt{[\log(\gamma_g-1)]^2+\pi^2}}\\ \tau_c^{gh}=\sqrt{\dfrac{\tau}{\gamma_h}}\end{cases} \tag{37}$$

Case E ($\varpi_1=\varpi_2=\sigma_3=0$): The global optimum, ($\zeta^{*f}$, τ_c^{*f}), is placed on the active constraint $\gamma_f-\mathrm{f}(\zeta,\ \tau_c)$. Solving the following equations will provide the optimum solutions:

$$\begin{cases}\gamma_f-\mathrm{f}(\zeta,\ \tau_c)=0\\ \dfrac{\partial \mathrm{f}(\zeta,\ \tau_c)}{\partial \tau_c}\dfrac{\partial \phi}{\partial \zeta}-\dfrac{\partial \mathrm{f}(\zeta,\ \tau_c)}{\partial \zeta}\dfrac{\partial \phi}{\partial \tau_c}=0\end{cases} \tag{38}$$

Case F ($\varpi_1=\sigma_2=\sigma_3=0$): The global optimum, ($\zeta^{gf}$, τ_c^{gf}), is on the vertex point delimited by $\gamma_g-\mathrm{g}(\zeta)=0$ and $\gamma_f-\mathrm{f}(\zeta,\ \tau_c)=0$. Solving the following equations will provide the optimum solutions:

$$\begin{cases}\zeta^{gf}=\zeta_{min}=-\dfrac{\log(\gamma_g-1)}{\sqrt{[\log(\gamma_g-1)]^2+\pi^2}}\\ \gamma_f-\mathrm{f}(\zeta_{min},\ \tau_c)=0\end{cases} \tag{39}$$

Case G ($\sigma_1=\sigma_3=\varpi_2=0$): The global optimum, ($\zeta^{fh}$, τ_c^{fh}), is on the acme point delimited by $\gamma_h-\mathrm{h}(\zeta,\ \tau_c)=0$ and $\gamma_f-\mathrm{f}(\zeta,\ \tau_c)=0$. Solving the following equations will provide the optimum solutions:

$$\begin{cases}\gamma_f-\mathrm{f}(\zeta,\ \tau_c)=0\\ \gamma_h-\mathrm{h}(\zeta,\ \tau_c)=0\end{cases} \tag{40}$$

Remark: Since integrating systems could be considered as a subset of FOPDT systems where both the process gain K and the process time constant τ with infinite values, the integrating system results can

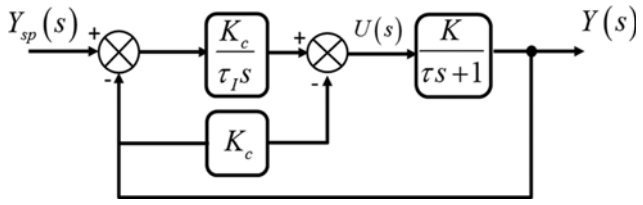

Fig. 2. Feedback diagram of a servo type-C PI controller for a first-order process.

be easily derived from the results presented in this paper, by setting both K and τ to sufficiently large values.

RELATIONSHIP BETWEEN THE IMC STRUCTURE AND TYPE-C PI CONTROL STRUCTURE

A type-C PI controller, also known as I-P controller, is a modified type of PID controller in which the set point is removed from the proportional term in order to avoid the initial quick on the manipulated variable for a step change in the set point. A typical I-P controller is represented in Fig. 2. This controller is integrated in the Smith predictor structure and represented in Fig. 3.

The closed loop transfer function of the system in Fig. 1 can be given as [13]

$$\mathrm{Y}=\frac{1}{\varepsilon\tau_c\tau_I\mathrm{s}^2+\varepsilon\tau_I\mathrm{s}+1}\mathrm{Y}_{sp}$$
$$\mathrm{U}=\frac{\frac{1}{\mathrm{K}}(\mathrm{s}\tau+1)}{\varepsilon\tau_c\tau_I\mathrm{s}^2+\varepsilon\tau_I\mathrm{s}+1}\mathrm{Y}_{sp} \tag{41}$$

With

$$\tau_c=\frac{\tau}{1+\mathrm{KK}_c};\ \varepsilon=\frac{1}{1-\frac{\tau_c}{\tau}} \tag{42}$$

To find the relationship between the type-C PI controller and the IMC parameters, their transfer function (closed loop) should be equal as given below:

$$\mathrm{Y}^*=\frac{1}{\tau_{c_{IMC}}^2\mathrm{s}^2+2\zeta_{IMC}\tau_{c_{IMC}}\mathrm{s}+1}\mathrm{Y}_{sp}=\frac{1}{\varepsilon\tau_c\tau_I\mathrm{s}^2+\varepsilon\tau_I\mathrm{s}+1}\mathrm{Y}_{sp}$$
$$\mathrm{U}=\frac{\tau\mathrm{s}+1}{\mathrm{K}}\frac{1}{\tau_{c_{IMC}}^2\mathrm{s}^2+2\zeta_{IMC}\tau_{c_{IMC}}\mathrm{s}+1}\mathrm{Y}_{sp}=\frac{\frac{1}{\mathrm{K}}(\mathrm{s}\tau+1)}{\varepsilon\tau_c\tau_I\mathrm{s}^2+\varepsilon\tau_I\mathrm{s}+1}\mathrm{Y}_{sp}(\mathrm{s}) \tag{43}$$

Eq. (43) yields

$$\begin{cases}\tau_{c_{IMC}}^2=\lambda_1=\varepsilon\tau_c\tau_I\\ 2\zeta_{IMC}\tau_{c_{IMC}}=\lambda_2=\varepsilon\tau_I\end{cases} \tag{44}$$

Eqs. (42) and (44) yield,

$$\mathrm{K}_c=\frac{1}{\mathrm{K}}\left(\frac{\lambda_2\tau}{\lambda_1}-1\right)=\frac{1}{\mathrm{K}}\left(\frac{2\zeta_{IMC}\tau_{c_{IMC}}\tau}{\tau_{c_{IMC}}^2}-1\right)$$
$$\tau_I=\lambda_2-\frac{\lambda_1}{\tau}=2\zeta_{IMC}\tau_{c_{IMC}}-\frac{\tau_{c_{IMC}}^2}{\tau} \tag{45}$$

With the relation in Eq. (45), the Smith predictor diagram in Fig. 3 is equivalent to the IMC diagram in Fig. 1.

SIMULATION STUDY

Without loss of generality, the simulation in this paper was obtained for the following FOPDT process:

$$\mathrm{G(s)}=\frac{10}{\mathrm{s}+1}\mathrm{e}^{-1.2s} \tag{46}$$

Fig. 4 shows the seven feasible cases of the constraints or restriction specifications. Depending on the constraint requirements in Table 1, the site of the global optimum can be inside the favorable region delimited by three restrictions (case A), on one active restriction (cases B, C, or E), or on the intersection of two restrictions (cases D, F, or G).

1. Time Responses Constraint Satisfaction

Figs. 5 and 6 display the feedback of the process variable, y(t), the manipulated variable u(t) and rate of change u′(t), for the seven possible cases listed in Table 1, for $\omega_y=\omega_u=0.5$. As shown in the figures, the proposed IMC filter parameters not only yield the opti-

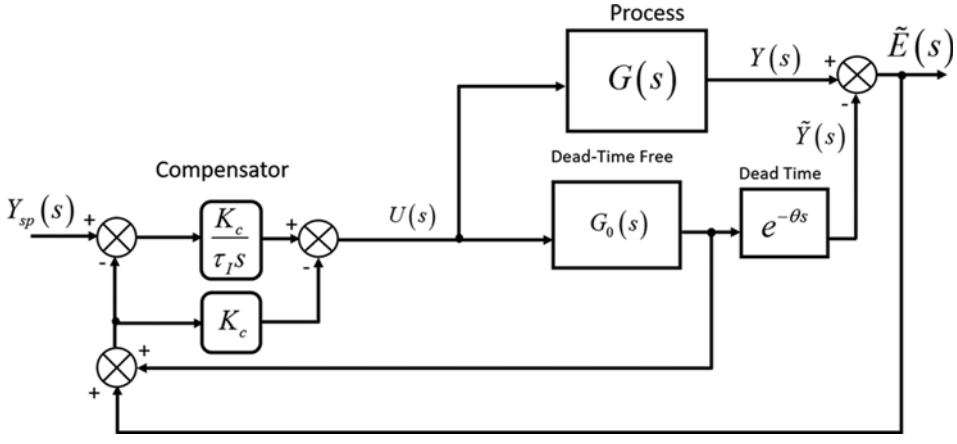

Fig. 3. Smith Predictor plus type-C PI controller.

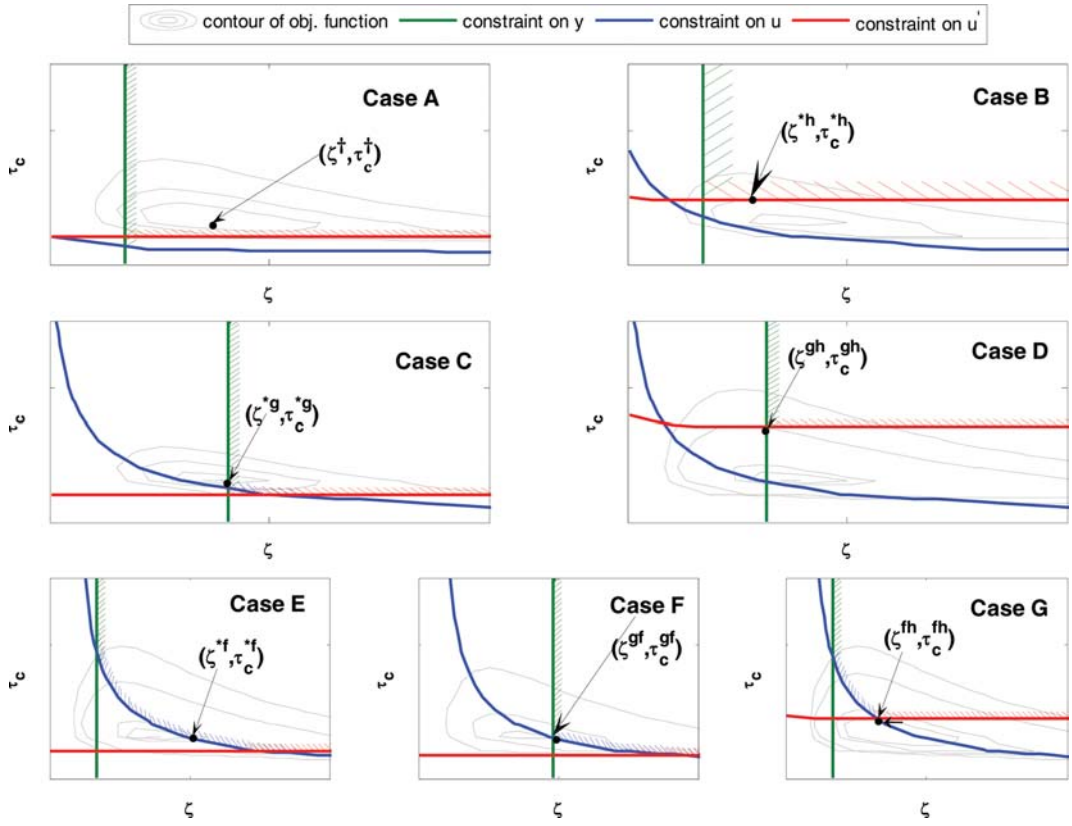

Fig. 4. Contours of the objective function and constraints for the seven possible optimal cases.

Table 1. Constraint specifications and resulting optimal IMC and PI parameters

Example	Case	Constraint specification			IMC parameters		PI parameters	
		y_{max}	u_{max}	u'_{max}	ζ	τ_c	K_c	τ_I
1	A	1.3	0.5	1.2	0.7246	0.3162	0.3583	0.3583
2	B	1.3	0.2	0.4	0.5477	0.5	0.1191	0.2977
3	C	1.01	0.5	1.2	0.8261	0.3017	0.4476	0.4075
4	D	1.09	0.5	0.2	0.6083	0.7071	0.0721	0.3603
5	E	1.3	0.15	1.2	0.9948	0.3181	0.5254	0.5317
6	F	1.05	0.15	1.2	0.69	0.4575	0.2016	0.4220
7	G	1.3	0.16	0.5	0.6310	0.4472	0.1822	0.3644

mal responses, but strictly satisfy the y_{max}, u_{max} and u'_{max} constraint specifications. Also, the Smith predictor parameters obtained from the IMC parameters lead to the same responses as that of the IMC, which proves the equivalency between the two structures, for the FOPDT process.

2. Effect of the Constraint Specifications on the Feasible Region

For a given constrained optimization problem, it is necessary to check the feasibility of a solution for any given constraint set before attempting to actually solve the optimal control problem. Eq. (35) show that the maximum allowable process variable, y_{max}, should be greater than ΔY_{sp} and less than $2\Delta Y_{sp}$. Eq. (A2) in the appendix shows that the maximum feasible/desirable value of the manipulated variable, u_{max} should not be less than the steady state value of the manipulated variable, $\Delta Y_{sp}/K$, whereas Eq. (A3) shows that the maximum feasible/desirable value of the rate of change of the manipulated variable, u'_{max}, can be chosen as smaller as possible, as long as it is a positive value. Fig. 7 shows the trend of the restrictions and viable region as the constraints specifications decrease. The constraints imposed by y_{max} in Eq. (19-1) lay a vertical line, the constraint imposed by u'_{max} in Eq. (19-3) lay a horizontal line, whereas the constraint imposed by u_{max} in Eq. (19-2) is a curve shape in (ζ, τ_c) space. As the y_{max}, u_{max} and u'_{max} specifications decrease, although the feasible region delimited through these constraints narrows down, the existence of feasible region is guaranteed, as long as the basic constraint requirements are met: $\Delta Y_{sp}<y_{max}<2\Delta Y_{sp}$, $u_{max}>(\Delta Y_{sp}/K)$, and $u'_{max}>0$.

3. Effect of the Process Parameters on the Extreme Point and Feasible Region

The shape along with the location of the constraints in (ζ, τ_c) space has an impact on the size of the feasible region with the vari-

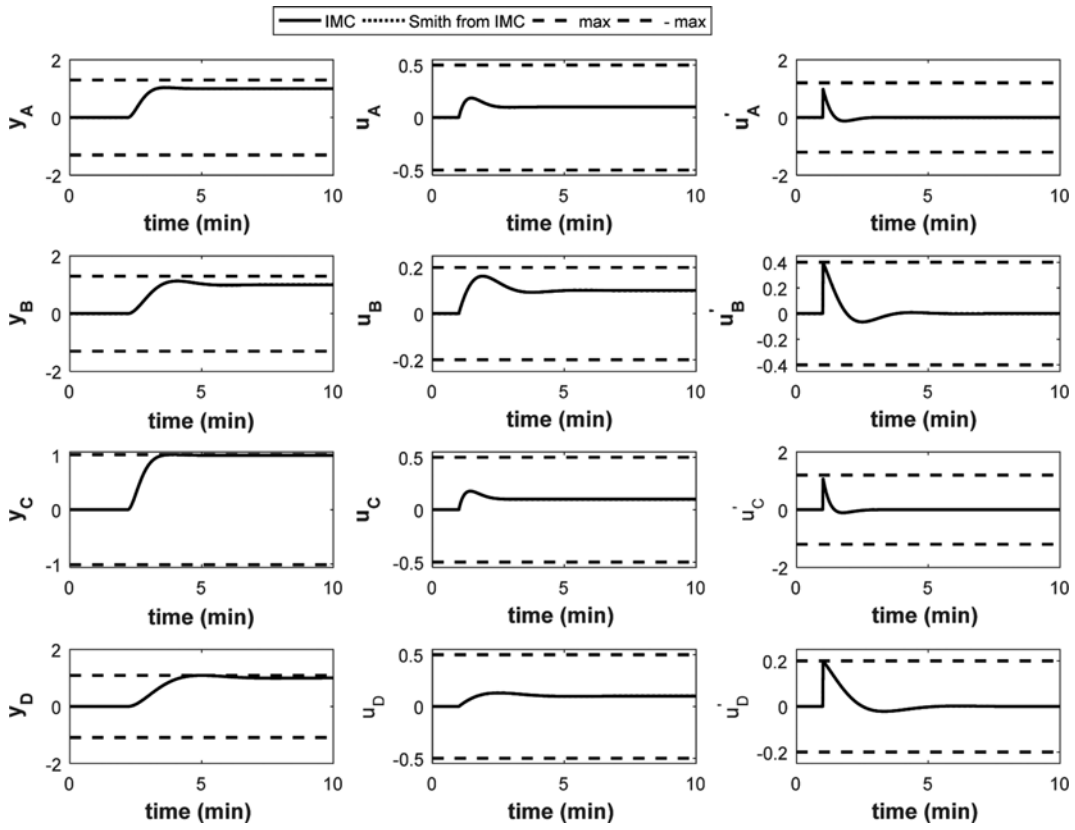

Fig. 5. Time response of the process, manipulated and rate of change of the manipulated variable for case A to case D.

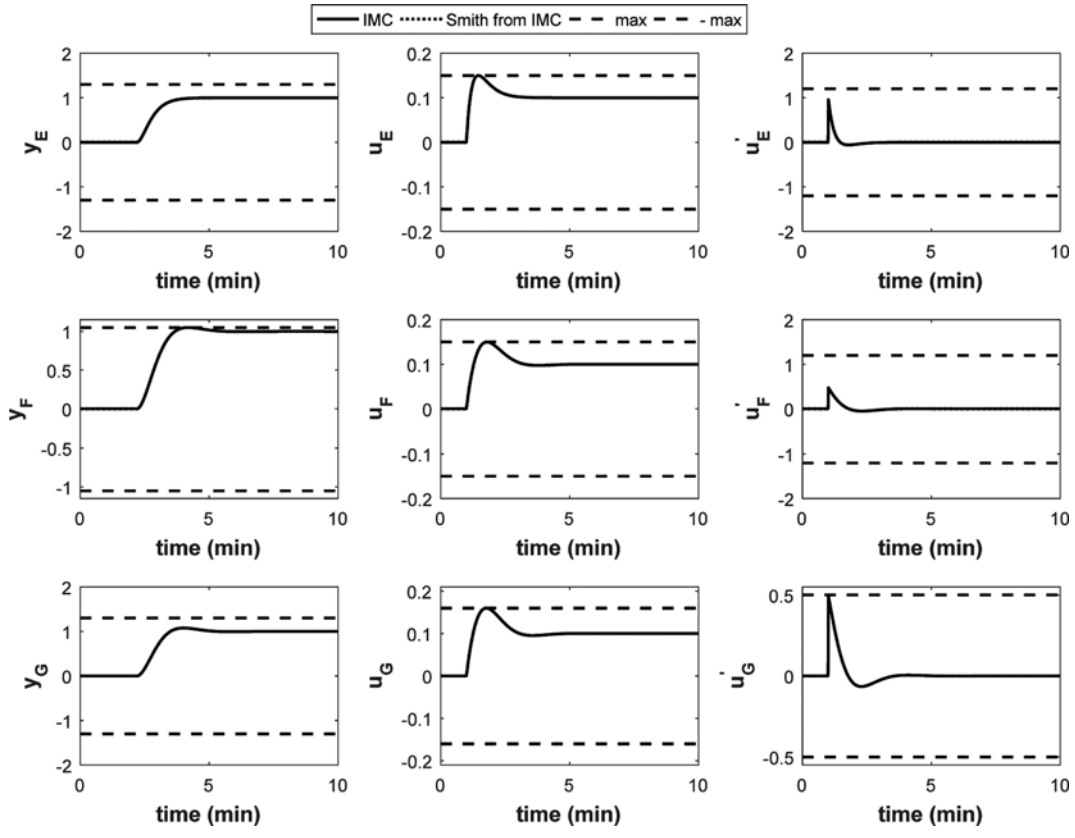

Fig. 6. Time response of the process, manipulated and rate of change of the manipulated variable for case E to case G.

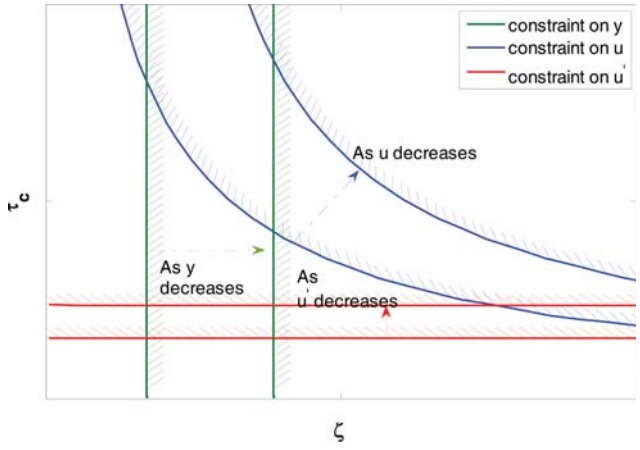

Fig. 7. Effect of the decrease of constraint specifications on the feasible region.

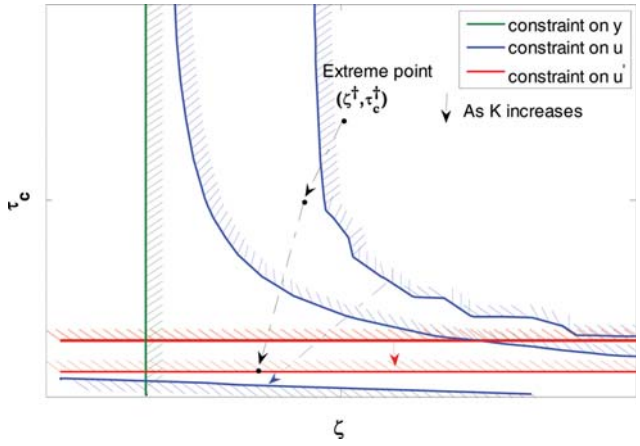

Fig. 8. Effect of the process gain on the trajectories of the extreme and the size of the feasible region.

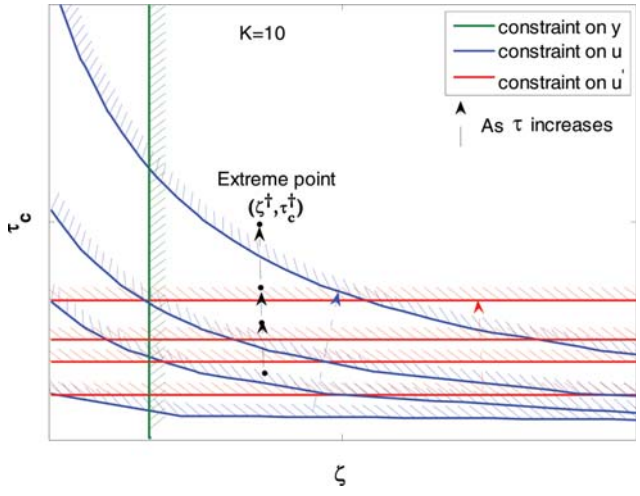

Fig. 9. Effect of the process time constant on the trajectories of the extreme and the size of the feasible region, for K=10.

ation of the process operating parameters. Fig. 8 shows the variation of the extreme point and constraint curves with the process

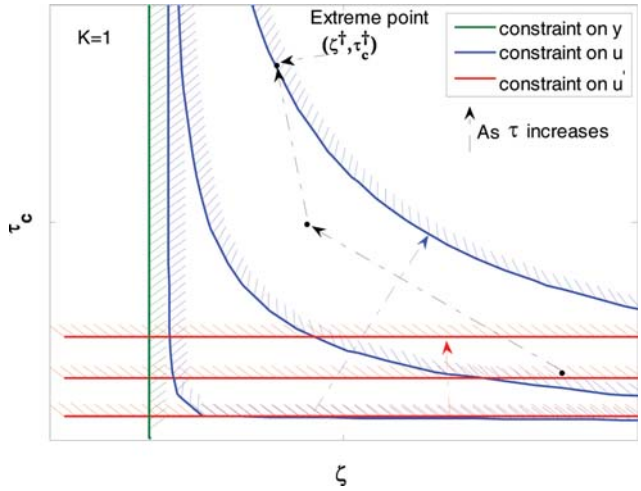

Fig. 10. Effect of the process time constant on the trajectories of the extreme and the size of the feasible region, for K=1.

gain, while Figs. 9 and 10 show the same curves as the time constant varies. As per increment in process gain, K, the global optimum of the IMC filter moves to a reduced left place in (ζ, τ_c) space, the constraint by u_{max} shifts to a lower position while stretching out, and the constraint by u'_{max} slowly shifts down. The constraint by u'_{max} also relatively alters from minimum to maximum position with respect to the constraint by u_{max}, as K increases. Therefore, for small values of the process gain, the optimal response is likely to be on the constraint imposed by u_{max}; that is, case E, then, as K increases, the optimal response is likely to shift from case E to case C (constrained by y_{max}) or case B (constrained by u'_{max}). In contrast, as shown by Figs. 9 and 10, shows the shifting of the maxima to a upper position and the two constraints move to a upper position in (ζ, τ_c) space, as the time constant, τ increases. In Fig. 9, K was set to 10, while in Fig. 10, K was decreased ten times and set to K=1. The main difference between the two figures is tha as τ increases, the optimum values of the IMC parameters shift up and almost vertically in Fig. 9, meaning that the optimal value of ζ is almost constant for K=10 and as τ increases, whereas in Fig. 10, for K=1, the optimal value of ζ decreases while the optimum value of τ_c increases. The other observation is that, as shown in Fig. 10, for smaller values of K and τ, one branch of the constraint set by u_{max} approaches the minimum value of ζ, ζ_{min}, delimited by the vertical constraint imposed by y_{max} and never cross that vertical, while the other branch of the constraint set by u_{max} is horizontal. This means that for smaller values of K and τ, the feasible region will be delimitated by the constraint by u_{max} and that by u'_{max}, and as τ increases by the constraint by u_{max} alone, as shown in Fig. 10. Therefore, the optimal response is possible to be constrained by u'_{max} initially, and further by y_{max} and/or u_{max} as τ increases further in case of Fig. 9, or constrained by u'_{max} and then only by u_{max} as τ increases further in case of Fig. 10. Note that the constraint by y_{max} does not depend on the process parameters.

4. Controller Robustness: Effect of Process Mismatch on the Control Design

To analyze the robustness of the system to external disturbances and/or plant-model mismatch, the worst-case plant-model mismatch

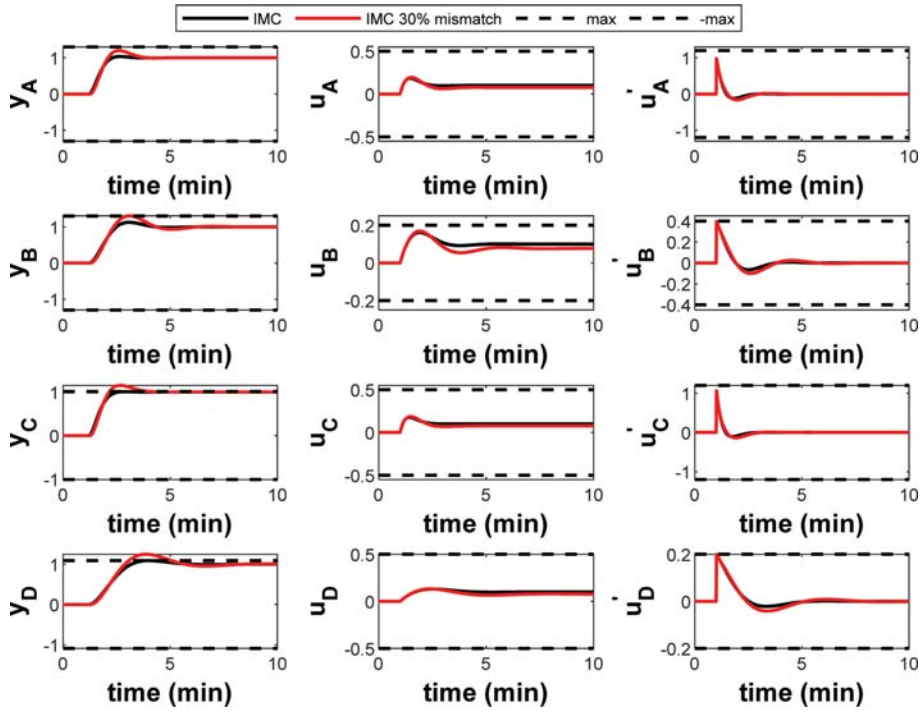

Fig. 11. Time response of the process, manipulated and rate of change of the manipulated variable for the plant-model mismatch of 30% for case A to case D.

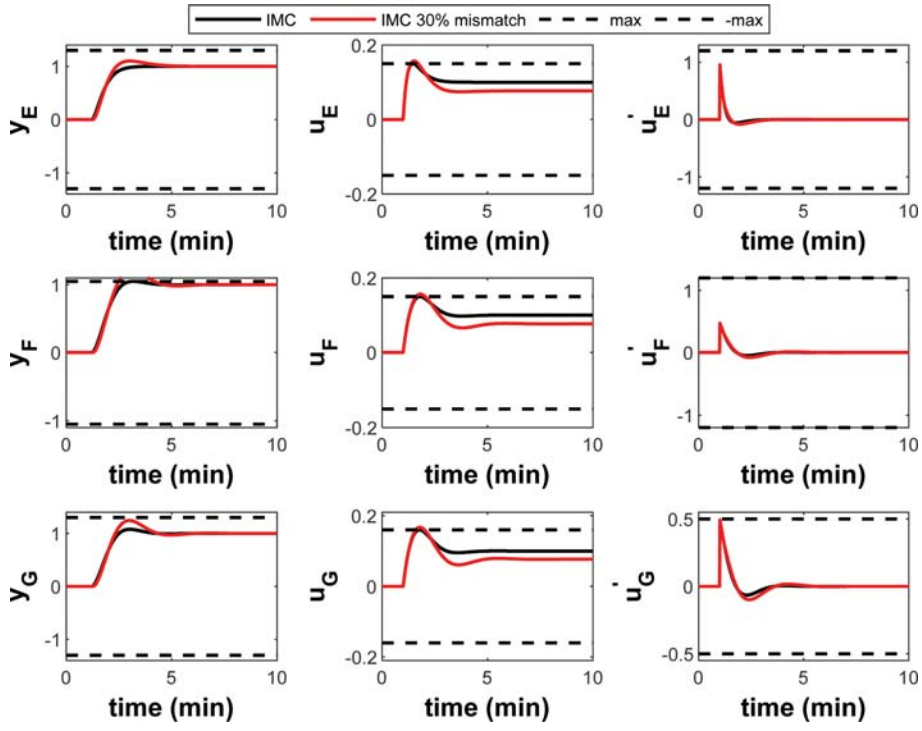

Fig. 12. Time response of the process, manipulated and rate of change of the manipulated variable for the plant-model mismatch of 30% for case E to case G.

scenario was simulated, where a percentage of perturbation was simultaneously introduced in the process gain parameters, the process time constant, and the dead-time. The optimal IMC controllers showed a good robustness against plant-model mismatch up to about 10%; thereafter, the process responses started to violate the constraints in some cases. Figs. 11 and 12 show the results of simulation for the model mismatch, when the percentage of the perturbation is 30%. As shown in these figures, the controller still strives to keep the con-

straints in some cases, like case B, where all the constraints on the process variable, the manipulated variable, and the rate of change of the manipulated variable are satisfied. In other cases, the controller failed to satisfy the constraints due to high level of plant mismatch.

CONCLUSIONS

An analytical design of a constrained optimal IMC controller was proposed. The proposed IMC controller successfully handled the control performance (minimization of the performance index) and satisfied the operational constraints. The proposed exact optimal IMC control parameters are directly connected to the plant parameters, which results in no trial and error required for the controller design. The feasible region of the constrained optimal problem could be graphically provided. The resulting constrained IMC control parameters were used to find the corresponding industrial constrained PI control parameters of a Smith predictor structure, and the results confirmed the equality between the IMC and the Smith predictor structure.

ACKNOWLEDGEMENT

This work was supported by the 2017 Yeungnam University Research Grant and by the Priority Research Centers Program through the National Research Foundation of Korea (NRF) funded by the Ministry of Education (2014R1A6A1031189).

NOTES

The authors declare no competing financial interest.

REFERENCES

1. P. L. T. Duong, L. Q. Minh, M. A. Qyyum and M. Lee, *Chem. Eng. Res. Des.*, **137**, 553 (2018).
2. W. Ali, P. L. T. Duong, M. A. Qyyum, A. Nawaz and M. Lee, *Comput. Aided* Chem. *Eng.*, **40**, 439 (2017).
3. D. Chen and D. E. Seborg, *Ind. Eng. Chem. Res.*, **41**, 4807 (2002).
4. D. E. Rivera, M. Morari and S. Skogestad, *Ind. Eng. Chem. Process Des. Dev.*, **25**, 252 (1986).
5. J. M. Vandeursen and J. A. Peperstraete, *Int. J. Control*, **62**, 983 (1995).
6. I. G. Horn, J. R. Arulandu, C. J. Gombas, J. G. VanAntwerp and R. D. Braatz, *Ind. Eng. Chem. Res.*, **35**, 3437 (1996).
7. P. V. G. K. Rao, M. V. Subramanyam and K. Satyaprasad, *Syst. Sci. Control Eng.*, **2**, 583 (2014).
8. P. S. Fruehauf, I.-L. Chien and M. D. Lauritsen, *ISA Trans.*, **33**, 43 (1994).
9. Z. Zhao, Z. Liu and J. Zhang, *J. Cent. South Univ. Technol.*, **18**, 1153 (2011).
10. K. G. Begum, A. S. Rao and T. K. Radhakrishnan, *ISA Trans.*, **68**, 223 (2017).
11. K. Liu, T. Shimizu, M. Inagaki and A. Ohkawa, *J. Chem. Eng. Japan*, **31**, 320 (1998).
12. M. Shamsuzzoha, M. Skliar and M. Lee, *Asia-Pacific J. Chem. Eng.*, **7**, 93 (2012).
13. H. C. T. Thu and M. Lee, *Korean J. Chem. Eng.*, **30**, 2151 (2013).

APPENDICES

Appendix A: Time Function y(t), u(t), u′(t)

$$y(t)=\begin{cases}\Delta Y_{sp}-\dfrac{\Delta Y_{sp}}{x}e^{-\frac{\zeta}{\tau_c}t}\left[\sin\left(x\dfrac{\zeta}{\tau_c}t\right)+x\cos\left(x\dfrac{\zeta}{\tau_c}t\right)\right] & \text{for } 0<\zeta<1\\ \Delta Y_{sp}-\dfrac{\Delta Y_{sp}}{\tau_c}e^{-\frac{1}{\tau_c}t}(t+\tau_c) & \text{for } \zeta=1\\ \Delta Y_{sp}-\dfrac{\Delta Y_{sp}}{x}e^{-\frac{\zeta}{\tau_c}t}\left[\sinh\left(x\dfrac{\zeta}{\tau_c}t\right)+x\cosh\left(x\dfrac{\zeta}{\tau_c}t\right)\right] & \text{for } \zeta>1\end{cases} \tag{A1}$$

$$u=\begin{cases}\dfrac{\Delta Y_{sp}}{K}-\dfrac{\Delta Y_{sp}}{K}e^{-\frac{\zeta}{\tau_c}t}\left[\cos\left(\dfrac{\zeta}{\tau_c}xt\right)+\dfrac{\zeta\tau_c-\tau}{\tau_c x\zeta}\sin\left(\dfrac{\zeta}{\tau_c}xt\right)\right] & \text{for } 0<\zeta<1\\ \dfrac{\Delta Y_{sp}}{K}-\dfrac{\Delta Y_{sp}}{K}e^{-\frac{\zeta}{\tau_c}t}\left(1+\dfrac{\tau_c-\tau}{\tau_c^2}t\right) & \text{for } \zeta=1\\ \dfrac{\Delta Y_{sp}}{K}-\dfrac{\Delta Y_{sp}}{K}e^{-\frac{\zeta}{\tau_c}t}\left[\cosh\left(\dfrac{\zeta}{\tau_c}xt\right)+\dfrac{\zeta\tau_c-\tau}{\tau_c x\zeta}\sinh\left(\dfrac{\zeta}{\tau_c}xt\right)\right] & \text{for } \zeta>1\end{cases} \tag{A2}$$

$$u'(t)=\begin{cases}\dfrac{\Delta Y_{sp}}{K}\dfrac{1}{\tau_c^2}e^{-\frac{\zeta}{\tau_c}t}\left[\dfrac{\tau_c-\zeta\tau}{\zeta x}\sin\left(\dfrac{\zeta}{\tau_c}xt\right)+\tau\cos\left(\dfrac{\zeta}{\tau_c}xt\right)\right] & \text{for } 0<\zeta<1\\ \dfrac{\tau\tau_c+(\tau_c-\tau)t}{K\tau_c^3}\Delta Y_{sp}e^{-\frac{1}{\tau_c}t} & \text{for } \zeta=1\\ \dfrac{\Delta Y_{sp}}{K}\dfrac{1}{\tau_c^2}e^{-\frac{\zeta}{\tau_c}t}\left[\dfrac{\tau_c-\tau\zeta}{\zeta x}\sinh\left(\dfrac{\zeta}{\tau_c}xt\right)+\tau\cosh\left(\dfrac{\zeta}{\tau_c}xt\right)\right] & \text{for } \zeta>1\end{cases} \tag{A3}$$

where

$$x=\begin{cases}\dfrac{\sqrt{\zeta^2-1}}{\zeta} & \text{for } \zeta>1\\ \dfrac{\sqrt{1-\zeta^2}}{\zeta} & \text{for } \zeta<1\end{cases} \tag{A4}$$

Appendix B: Peak Value of y(t), u(t), u′(t)

The peak value of the process variable can be derived by solving peak time t_{ypeak} for which $y'(t)=0$ and substituting t_{ypeak} in y(t). After some mathematical manipulations and reductions, the peak time of the process variable is found as

$$t_{ypeak}=\begin{cases}\dfrac{\pi\tau_c}{x\zeta} & \text{for } 0<\zeta<1\\ \infty & \text{for } \zeta\geq 1\end{cases} \tag{B1}$$

And the peak value of the process variable is found as

$$|y_{peak}|=|\Delta Y_{sp}|g(\zeta) \tag{B2}$$

with

$$g(\zeta)=\begin{cases}1+e^{-\frac{\pi}{x}} & \text{for } 0<\zeta<1\\ 1 & \text{for } \zeta\geq 1\end{cases} \tag{B3}$$

The peak value of the manipulated variable can be derived by solving peak time t_{upeak} for which u′(t)=0 and substituting t_{upeak} in u(t). After some mathematical manipulations and reductions, the peak time of the manipulated variable can be found as

$$t_{upeak}=\begin{cases}\frac{\tau_c}{x\zeta}\left[\tan^{-1}\left(\frac{\tau\zeta x}{\zeta\tau-\tau_c}\right)+\pi\right] & \text{for } \zeta<1 \text{ and } \tau_c>\tau\zeta\\ \frac{\tau_c}{x\zeta}\tan^{-1}\left(\frac{\tau\zeta x}{\zeta\tau-\tau_c}\right) & \text{for } \zeta<1 \text{ and } \tau_c\leq\tau\zeta\\ +\infty & \text{for } \zeta>1 \text{ and } \tau_c\geq\zeta\tau(1-x)\\ \frac{\tau_c}{\zeta x}\tanh^{-1}\left(\frac{\tau\zeta x}{\zeta\tau-\tau_c}\right) & \text{for } \zeta>1 \text{ and } \tau_c<\zeta\tau(1-x)\\ +\infty & \text{for } \zeta=1 \text{ and } \tau_c\geq\tau\\ \frac{\tau\tau_c}{\tau-\tau_c} & \text{for } \zeta=1 \text{ and } \tau_c<\tau\end{cases} \tag{B4}$$

The peak value of the manipulated variable can be found as

$$|u_{peak}|=\left|\frac{\Delta Y_{sp}}{K}\right|f(\zeta,\ \tau_c) \tag{B5}$$

with

$$f(\zeta,\ \tau_c)=\begin{cases}1 & \text{for } \zeta>1 \text{ and } \tau_c\geq\zeta\tau(1-x)\\ 1+\frac{1}{\tau_c}\sqrt{\tau^2-2\zeta\tau\tau_c+\tau_c^2}\,e^{-\frac{1}{x}tanh^{-1}\left(\frac{\tau\zeta x}{\zeta\tau-\tau_c}\right)} & \text{for } \zeta>1 \text{ and } \tau_c\leq\zeta\tau(1-x)\\ 1+\frac{1}{\tau_c}\sqrt{\tau^2-2\zeta\tau_c\tau+\tau_c^2}\,e^{-\frac{1}{x}tan^{-1}\left(\frac{\tau\zeta x}{\zeta\tau-\tau_c}\right)-\frac{\pi}{x}} & \text{for } \zeta<1 \text{ and } \tau_c>\tau\zeta\\ 1+\frac{1}{\tau_c}\sqrt{\tau^2-2\zeta\tau_c\tau+\tau_c^2}\,e^{-\frac{1}{x}tan^{-1}\left(\frac{\tau\zeta x}{\zeta\tau-\tau_c}\right)} & \text{for } \zeta<1 \text{ and } \tau_c\leq\tau\zeta\\ 1 & \text{for } \zeta=1 \text{ and } \tau_c\geq\tau\\ 1+\left(\frac{\tau-\tau_c}{\tau_c}\right)e^{-\frac{\tau}{\tau-\tau_c}} & \text{for } \zeta=1 \text{ and } \tau_c<\tau\end{cases} \tag{B6}$$

The peak value of the rate of change of the manipulated variable can be derived by solving peak time $t_{u'peak}$ for which u″(t)=0 and substituting $t_{u'peak}$ in u′(t). After some mathematical manipulations and reductions, the theoretical peak time of the rate of change of the manipulated variable can be found as

$$t_{u'peak}=\begin{cases}\frac{\tau_c}{\zeta x}\left\{\tan^{-1}\left[\frac{\zeta x(\tau_c-2\tau\zeta)}{\zeta\tau_c-\tau(2\zeta^2-1)}\right]+\pi\right\} & \text{for } 0<\zeta\leq\frac{1}{\sqrt{2}} \text{ and } \tau_c<2\tau\zeta\\ \frac{\tau_c}{\zeta x}\tan^{-1}\left[\frac{\zeta x(\tau_c-2\tau\zeta)}{\zeta\tau_c-\tau(2\zeta^2-1)}\right] & \text{for } 0<\zeta\leq\frac{1}{\sqrt{2}} \text{ and } \tau_c\geq2\tau\zeta\\ \frac{\tau_c}{\zeta x}\tan^{-1}\left[\frac{\zeta x(\tau_c-2\tau\zeta)}{\zeta\tau_c-\tau(2\zeta^2-1)}\right] & \text{for } \frac{1}{\sqrt{2}}<\zeta<1 \text{ and } \tau_c\in[0,\ \tau_{c_2}]\cup[\tau_{c_1}\rightarrow[\\ \frac{\tau_c}{\zeta x}\left\{\tan^{-1}\left[\frac{\zeta x(\tau_c-2\tau\zeta)}{\zeta\tau_c-\tau(2\zeta^2-1)}\right]+\pi\right\} & \text{for } \frac{1}{\sqrt{2}}<\zeta<1 \text{ and } \tau_c\in\,]\tau_{c_2},\ \tau_{c_1}]\\ +\infty & \text{for } \zeta>1 \text{ and } \tau_c\geq\tau_{c_3}\\ \frac{\tau_c}{x\zeta}\tanh^{-1}\left[\frac{\zeta x(\tau_c-2\tau\zeta)}{\zeta\tau_c-\tau(2\zeta^2-1)}\right] & \text{for } \zeta>1 \text{ and } \tau_c<\tau_{c_3}\\ +\infty & \text{for } \zeta=1 \text{ and } \tau_c\geq\tau_{c_3}=\tau\\ \frac{\tau_c(\tau_c-2\tau)}{\tau_c-\tau} & \text{for } \zeta=1 \text{ and } \tau_c<\tau_{c_3}=\tau\end{cases} \tag{B7}$$

with

$$\tau_{c_1}=2\tau\zeta;\ \tau_{c_2}=\tau\left(\frac{2\zeta^2-1}{\zeta}\right);\ \tau_{c_3}=2\tau\zeta-\frac{\tau}{\zeta(1-x)} \tag{B8}$$

The theoretical peak value of the rate of change of the manipulated variable can be found as

$$|u'_{peak\,0}|=\left|\frac{\Delta Y_{sp}}{K}\right|h(\zeta,\ \tau_c) \tag{B9}$$

where the theoretical values of $h(\zeta,\ \tau_c)$ are given as

$$h(\zeta,\ \tau_c)=\begin{cases}\frac{\sqrt{\tau_c^2-2\tau\tau_c\zeta+\tau^2}}{\tau_c^2}e^{-\frac{1}{x}\left\{tan^{-1}\left[\frac{\zeta x(\tau_c-2\tau\zeta)}{\zeta\tau_c-\tau(2\zeta^2-1)}\right]+\pi\right\}} & \text{for } 0<\zeta\leq\frac{1}{\sqrt{2}} \text{ and } \tau_c<2\tau\zeta\\ =\frac{\sqrt{\tau_c^2-2\tau\tau_c\zeta+\tau^2}}{\tau_c^2}e^{-\frac{1}{x}tan^{-1}\left[\frac{\zeta x(\tau_c-2\tau\zeta)}{\zeta\tau_c-\tau(2\zeta^2-1)}\right]} & \text{for } 0<\zeta\leq\frac{1}{\sqrt{2}} \text{ and } \tau_c\geq2\tau\zeta\\ \frac{\sqrt{\tau_c^2-2\tau\tau_c\zeta+\tau^2}}{\tau_c^2}e^{-\frac{1}{x}tan^{-1}\left[\frac{\zeta x(\tau_c-2\tau\zeta)}{\zeta\tau_c-\tau(2\zeta^2-1)}\right]} & \text{for } \frac{1}{\sqrt{2}}<\zeta<1 \text{ and } \tau_c\in[0,\ \tau_{c_2}]\cup[\tau_{c_1}\rightarrow[\\ \frac{\sqrt{\tau_c^2-2\tau\tau_c\zeta+\tau^2}}{\tau_c^2}e^{-\frac{1}{x}\left\{tan^{-1}\left[\frac{\zeta x(\tau_c-2\tau\zeta)}{\zeta\tau_c-\tau(2\zeta^2-1)}\right]+\pi\right\}} & \text{for } \frac{1}{\sqrt{2}}<\zeta<1 \text{ and } \tau_c\in\,]\tau_{c_2},\ \tau_{c_1}]\\ 0 & \text{for } \zeta>1 \text{ and } \tau_c\geq\tau_{c_3}\\ \frac{\sqrt{\tau_c^2-2\tau\tau_c\zeta+\tau^2}}{\tau_c^2}e^{-\frac{1}{x}tanh^{-1}\left[\frac{\zeta x(\tau_c-2\tau\zeta)}{\zeta\tau_c-\tau(2\zeta^2-1)}\right]} & \text{for } \zeta>1 \text{ and } \tau_c<\tau_{c_3}\\ 0 & \text{for } \zeta=1 \text{ and } \tau_c\geq\tau_{c_3}=\tau\\ \frac{\tau-\tau_c}{\tau_c^2}e^{-\frac{\tau_c-2\tau}{\tau_c-\tau}} & \text{for } \zeta=1 \text{ and } \tau_c<\tau_{c_3}=\tau\end{cases} \tag{B10}$$

To have the actual peak $|u'_{peak}|$ of the rate of change of the manipulated variable, the theoretical peak $|u'_{peak\,0}|$ in Eq. (B9), and the initial value of the rate of change of the manipulated variable, $|u'(0)|$, should be compared. If $|u'_{peak\,0}|<|u'(0)|$ then $|u'(0)|$ is the actual peak of $|u'(t)|$ since the theoretical peak in this case is not the actual peak. If $|u'_{peak\,0}|\geq|u'(0)|$ then $|u'_{peak\,0}|$ is the actual peak of $|u'(t)|$. The actual peak value of the rate of change of the manipulated variable can be found as

$$|u'_{peak}|=\left|\frac{\Delta Y_{sp}}{K}\right|h(\zeta,\ \tau_c) \tag{B11}$$

with

$$h(\zeta,\ \tau_c)=\frac{\tau}{\tau_c^2} \tag{B12-1}$$

under the following conditions

$$\begin{aligned}
&0<\zeta\leq\frac{1}{\sqrt{2}} \text{ and } \tau_c<2\tau\zeta \text{ or}\\
&0<\zeta\leq\frac{1}{\sqrt{2}} \text{ and } \tau_c\geq 2\tau\zeta \text{ and } h_0(\zeta,\ \tau_c)\tau_c^2<\tau \text{ or}\\
&\frac{1}{\sqrt{2}}<\zeta<1 \text{ and } (0<\tau_c\leq\tau_{c_2} \text{ or } \tau_c\geq\tau_{c_1}) \text{ and } h_0(\zeta,\ \tau_c)\tau_c^2<\tau \text{ or}\\
&\frac{1}{\sqrt{2}}<\zeta<1 \text{ and } \tau_{c_2}<\tau_c\leq\tau_{c_1} \text{ or}\\
&\zeta\geq 1 \text{ and } \forall\tau_c
\end{aligned} \tag{B12-2}$$

or

$$h(\zeta,\ \tau_c)=h_0(\zeta,\ \tau_c)=\frac{\sqrt{\tau_c^2-2\tau\tau_c\zeta+\tau^2}}{\tau_c^2}e^{-\frac{1}{x}\tan^{-1}\left[\frac{\zeta x(\tau_c-2\tau\zeta)}{\zeta\tau_c-\tau(2\zeta^2-1)}\right]} \tag{B12-3}$$

under the following conditions

$$\begin{aligned}
&\text{for } 0<\zeta\leq\frac{1}{\sqrt{2}} \text{ and } \tau_c\geq 2\tau\zeta \text{ and } h_0(\zeta,\ \tau_c)\tau_c^2\geq\tau\\
&\text{for } \frac{1}{\sqrt{2}}<\zeta<1 \text{ and } (0<\tau_c\leq\tau_{c_2} \text{ or } \tau_c\geq\tau_{c_1}) \text{ and } h_0(\zeta,\ \tau_c)\tau_c^2\geq\tau
\end{aligned} \tag{B12-4}$$

with τ_{c_1} and τ_{c_2} are given in Eq. (B8)